

On the Traffic Impacts of Optimally Controlled Connected and Automated Vehicles

Liuhui Zhao, Andreas A. Malikopoulos, Jackeline Rios-Torres

Abstract—The implementation of connected and automated vehicle (CAV) technologies enables a novel computational framework for real-time control actions aimed at optimizing energy consumption and associated benefits. Several research efforts reported in the literature to date have proposed decentralized control models to optimize vehicle trajectories in various traffic scenarios, e.g., highway on-ramps, intersections, and roundabouts. However, the impact of optimally controlled CAVs on the performance of a transportation network has not been thoroughly analyzed yet. In this paper, we apply a decentralized optimal control framework in a transportation network and compare its performance to a baseline scenario consisting of human-driven vehicles. We show that introducing of CAVs yields radically improved roadway capacity and network performance. Especially when taking into account shorter time headways enabled by the CAVs, the framework results in a non-stopping flow while addressing traffic congestion.

I. INTRODUCTION

Urban intersections, merging roadways, roundabouts, and speed reduction zones along with the driver responses to various disturbances [1] are the primary sources of bottlenecks that contribute to traffic congestion [2]. Connectivity and automation in vehicles provide the most intriguing opportunity for enabling users to better monitor transportation network conditions and make better operating decisions. However, investigating the impact of connected and automated vehicles (CAVs) on a transportation network and related implications on mobility and safety has been of great concern in recent studies [3].

Liuhui Zhao and Andreas A. Malikopoulos are with the Department of Mechanical Engineering, University of Delaware, Newark, DE 19716 USA; Jackeline Rios-Torres is with Oak Ridge National Laboratory, Oak Ridge, TN 37830 USA (emails: lzhao@udel.edu, andreas@udel.edu; riosstorresj@ornl.gov).

Several research efforts have been reported in the literature proposing different approaches on coordinating CAVs at different transportation segments, e.g., intersections, roundabouts, merging roadways, speed reduction zones, with the intention to improve traffic flow. Kachroo and Li [4] proposed a longitudinal and lateral controller to guide the vehicle until the merging maneuver is completed. Other efforts have focused on developing a hybrid control aimed at keeping a safe headway between the vehicles in the merging process [4], [5], or developing three levels of assistance for the merging process to select a safe space for the vehicle to merge [6]. In 2004, Dresner and Stone [7] proposed the use of the reservation scheme to control a single intersection of two roads with vehicles traveling with similar speed on a single direction on each road, i.e., no turns are allowed. Since then, numerous approaches have been reported in the literature [8]–[10], to achieve safe and efficient control of traffic through intersections including extensions of the reservation scheme in [7]. Some approaches have focused on coordinating vehicles at intersections to improve the travel flow [11]–[16]. Lee and Park [17] studied intersection coordination in a connected and automated environment where a phase conflict map is used to remove stop-and-go traffic signals, later on, an extended study [18] focused on the case of urban corridor that consists of multiple intersections. The simulation results revealed significant improvements in network performance in terms of travel time and fuel consumption. Most recently, [19] presented an approach for automated on-ramp merging and gap development considering vehicle speed constraints. A detailed discussion of the research efforts in this area can be found in [3], [20].

In earlier work, a decentralized optimal control framework was established for coordinating online CAVs in different transportation segments. A closed-form, analytical solution was presented and tested in different transportation scenarios in [21]–[23] for

coordinating online CAVs [24]–[29]. Most recently, Rios-Torres and Malikopoulos [30] discussed the traffic and fuel consumption impacts of partial penetration of CAVs for a highway on-ramp scenario. In previous studies, we discussed the potential benefits of optimally coordinated CAVs in a corridor such that stop-and-go driving is eliminated. However, there is still not clear how a group of optimally controlled CAVs changes the traffic patterns in a traffic network. In this paper, we explore the impact of our previously proposed optimal coordination framework for CAVs in a corridor under different traffic conditions. Specifically, we identify the benefits as well as the limitations of the optimally controlled CAVs in a transportation network.

The structure of the paper is organized as follows. In Section II, we introduce the optimal control framework applied in the study. We present the simulation evaluation framework and the traffic scenarios to be conducted in Section III. We provide the evaluation results in Section IV and concluding remarks are presented in Section V.

II. OPTIMAL CONTROL FRAMEWORK

We consider a *conflict zone* where traffic from two different roadways may cause potential lateral collisions, indicated in red in Fig. 1. Before the entry of the conflict zone, there is a *control zone* and a coordinator that can communicate with the vehicles traveling inside the control zone. Note that the coordinator is not involved in any decision of the vehicles. The length of the control zone is L , which is adjustable.

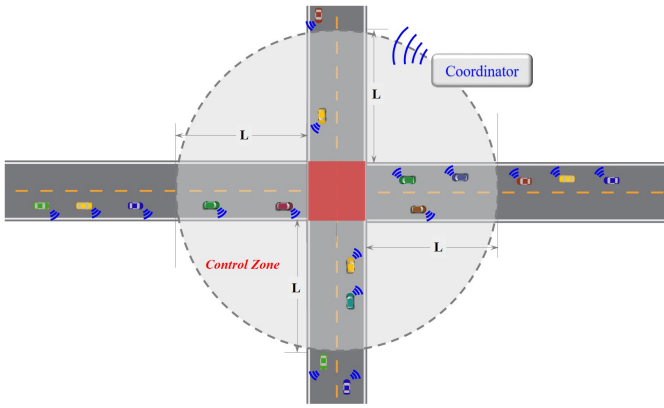


Fig. 1: An intersection with optimally controlled CAVs.

We consider a number of CAVs $N(t) \in \mathbb{N}$, where $t \in \mathbb{R}^+$ is the time, entering the control zone. Let

$\mathcal{N}(t) = 1, \dots, N(t)$ be a queue of vehicles in the control zone. The dynamics of each vehicle $i, i \in \mathcal{N}(t)$, are represented with a state equation

$$\dot{x}(t) = f(t, x_i, u_i), \quad x_i(t_i^0) = x_i^0, \quad (1)$$

where $x_i(t), u_i(t)$ are the state of the vehicle and control input, t_i^0 is the time that vehicle i enters the control zone, and x_i^0 is the value of the initial state. For simplicity, we model each vehicle as a double integrator, i.e., $\dot{p}_i = v_i(t)$ and $\dot{v}_i = u_i(t)$, where $p_i(t) \in \mathcal{P}_i, v_i(t) \in \mathcal{V}_i$, and $u_i(t) \in \mathcal{U}_i$ denote the position, speed, and acceleration/deceleration (control input) of each vehicle i . Let $x_i(t) = [p_i(t) \ v_i(t)]^T$ denotes the state of each vehicle i , with initial value $x_i^0(t) = [0 \ v_i^0(t)]^T$, taking values in the state space $\mathcal{X}_i = \mathcal{P}_i \times \mathcal{V}_i$. The sets $\mathcal{P}_i, \mathcal{V}_i$, and $\mathcal{U}_i, i \in \mathcal{N}(t)$, are complete and totally bounded subsets of \mathbb{R} . The state space \mathcal{X}_i for each vehicle i is closed with respect to the induced topology on $\mathcal{P}_i \times \mathcal{V}_i$ and thus, it is compact.

To ensure that the control input and vehicle speed are within a given admissible range, the following constraints are imposed.

$$u_{min} \leq u_i(t) \leq u_{max}, \text{ and} \quad (2)$$

$$0 \leq v_{min} \leq v_i(t) \leq v_{max}, \quad \forall t \in [t_i^0, t_i^f]$$

where u_{min}, u_{max} are the minimum deceleration and maximum acceleration respectively, and v_{min}, v_{max} are the minimum and maximum speed limits respectively. t_i^0 is the time that vehicle i enters the control zone, t_i^f is the time that vehicle i exits the conflict zone.

To ensure the absence of rear-end collision of two consecutive vehicles traveling on the same lane, the position of the preceding vehicle should be greater than, or equal to the position of the following vehicle plus a predefined safe distance $\delta_i(t)$, where $\delta_i(t)$ is proportional to the speed of vehicle i , $v_i(t)$. Thus, we impose the rear-end safety constraint

$$s_i(t) = p_k(t) - p_i(t) \geq \delta_i(t), \quad \forall t \in [t_i^0, t_i^f] \quad (3)$$

where vehicle k is immediately ahead of i on the same lane.

We consider the problem of minimizing the control input (acceleration/deceleration) for each vehicle i from the time t_i^0 that the vehicle enters the control zone until the time t_i^f that it exits the control zone. Thus, we

formulate the following optimization problem for each vehicle in the queue $\mathcal{N}(t)$

$$\min_{u_i} \frac{1}{2} \int_{t_i^0}^{t_i^f} u_i^2(t) dt \quad (4)$$

Subject to : (1), (2) $\forall i \in \mathcal{N}(t)$.

In this study, we apply the same decentralized optimal control framework as developed earlier in [23], [24], [28] and the analytical solution without considering the state and control constraints for the control of CAVs. The solution of the constrained problem at a single intersection was presented in [25].

III. SIMULATION EVALUATION

A. Simulation Environment

To compare network performance between conventional human-driven vehicles, uncontrolled automated vehicles (AVs), and optimally controlled CAVs, we create a simulation network in PTV VISSIM environment in Newark, Delaware area, which includes two signalized intersections (#1 and #2 in Fig. 2, two-lane each direction with dedicated left-turn and right-turn lanes at both intersections, one-lane on southbound at intersection #2), an unsignalized intersection between #1 and #2, and a major interchange (#3 in Fig. 2, four-lane each direction, two separated ez-pass only lanes on westbound that we do not consider in the simulation network). In terms of network size, the east-west road segment is approximately 2 km, and the north-south segment is about 2.2 km. We obtain hourly traffic information from 2017 annual average daily traffic report published by Delaware Department of Transportation [31], and simulate the morning peak hour (i.e., 8:00AM - 9:00AM) traffic. The traffic signal timings are optimized based on current network traffic condition (75 s cycle length for intersection 2 and 90 s cycle length for intersection 1) for the base case.

Specifically, for simulating human-driven vehicles, we apply the Wiedemann car following model [32] that is adopted in VISSIM, relating the minimum safe distance as a function of standstill distance and time headway [33]. For this study, the default 1.5 m standstill distance and 1.2 s time headway are set for simulating the human drivers' car following behavior. Acknowledging that more AVs are on road nowadays, VISSIM adapts its car following model to simulate the

AV's driving behavior through adjusting the variation in vehicle acceleration and following distance accordingly. Besides these adjustment, we adopt 0.9 s time headway to reflect the capability of an AV to follow a leading vehicle closer.

As discussed in the previous section, under optimal control operation, each CAV inside the control zone determines its own optimal acceleration profile to drive through the conflict zone smoothly without stop-and-go behavior. Once a vehicle exits an intersection or a merging area, the control algorithm is deactivated such that the vehicle follows any leading vehicle based on the Wiedemann car following model. We consider a control length of 150 m for CAV controlling. In correspondence with different driving behavior between human-driven vehicles and AVs, we apply two different time headway settings (i.e., 0.9 s and 1.2 s) in our optimal control algorithm for fair comparison with human-driven vehicles and AVs (Table I).

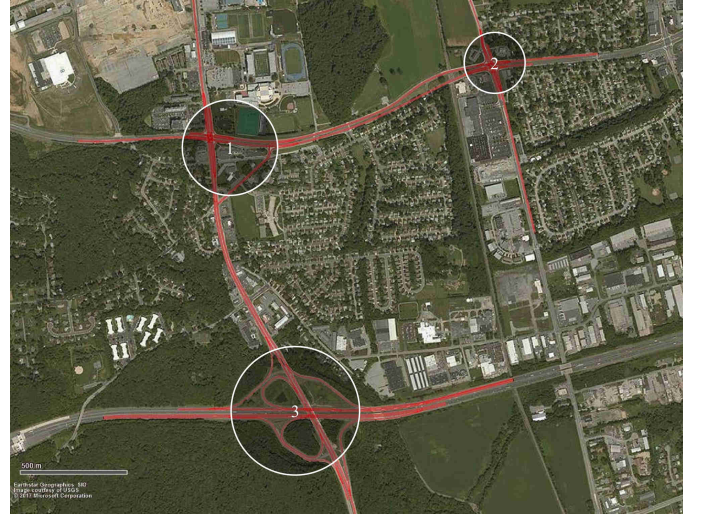


Fig. 2: Study area.

IV. EVALUATION RESULTS

A. Base case with existing traffic demand

In one hour simulation period, there is approximately 12,000 vehicles entering the network, half of which is served by the interchange. Traffic data is collected every 60 s and vehicle trajectory data is collected every 1 s.

Consider that there are both local and highway segments in the study network, we collect individual

TABLE I: Simulation settings for different scenarios.

Scenario	Vehicle Type	Headway (s)	Control Zone Length (m)	Signal Controller
1	Uncontrolled Human-driven Vehicle	1.2	-	Fixed-time
2	Uncontrolled AV	0.9	-	Fixed-time
3	Controlled CAV (vs. human-driven)	1.2	150	Disabled
4	Controlled CAV (vs. AV)	0.9	150	Disabled

vehicle trajectories to analyze vehicle behavior on different routes and try to understand how the optimal control framework affects different groups of traffic. We categorize the routes into four groups based on the origin and destination road types: a) local traffic, i.e., both origin and destination roads are arterial; b) highway traffic, i.e., both origin and destination roads are highway; c) local to highway; and d) highway to local. The average travel distances for the four groups are 1.7 km, 1.5 km, 1.7 km, and 2.0 km, respectively.

For all the vehicles during the simulation period, we plot the vehicle following distance distribution under four scenarios (Fig. 3). Due to a shorter vehicle headway, i.e., 0.9 s, enabled by AVs, we can see that the vehicles follow leading vehicles much more closely (Scenario 2 vs. Scenario 4). According to Wiedemann model, vehicle following distance is positively related to vehicle speed. When a vehicle stops, the following distance to its leading vehicle is the stand-still distance, i.e., 1.5 m. Therefore, in general, local traffic would have more short following distance than highway traffic, e.g., Group a vs. Group b in Fig. 3a.

With the optimal control framework, the following distances are increased for all four traffic groups. There are two major reasons: (1) vehicle movements inside the control zones are optimally controlled such that the desired time headway could be guaranteed at each conflict zone; and (2) vehicle stopping at each conflict zone is eliminated as a result of coordination (shown in Table II). Furthermore, looking into vehicle lane change behavior, we find that the average number of lane change is reduced under Scenarios 3 and 4. Especially, almost a half of the total lane changes is eliminated for highway traffic, e.g., an average of 0.34 under scenario 1 vs. 0.18 under scenario 3 in Table II. For human-driven vehicles or uncontrolled AVs, it is usually the case that mainline vehicles (especially those on the travel lanes closest to the ramp) would prefer to

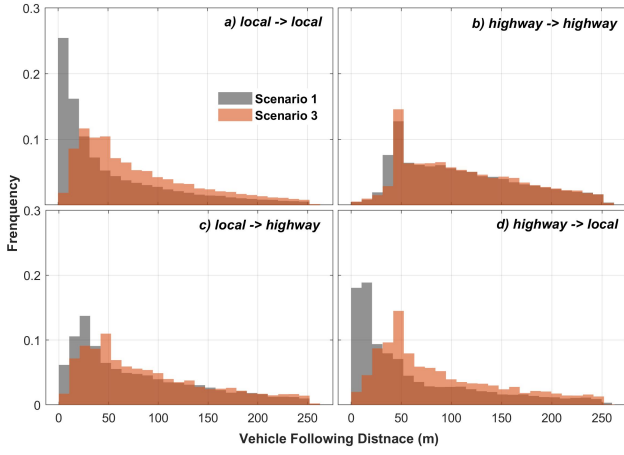
make lane changes near ramps to avoid interruptions from ramp vehicles. Whereas, under optimal control, all CAVs coordinate with each other such that lane change is not necessary for mainline vehicles. As a result, the number of lane changes is significantly reduced in the network. Through eliminating stop-and-go driving and reducing the number of lane changes, the optimal control framework not only improves traffic mobility, i.e., reduced average travel time as shown in Table II, but also enhances safety in the network.

TABLE II: Trip performance measurements under different scenarios.

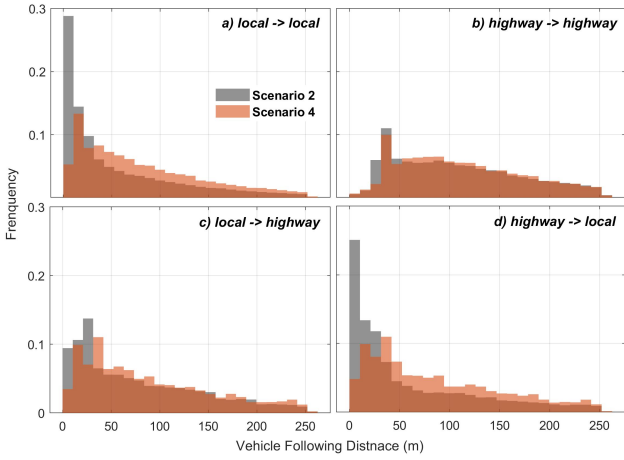
Scenario	1	2	3	4	1	2	3	4
Average Travel Time (s)				Average Speed (m/s)				
local->local	126.8	123.9	92.2	90.7	13.6	13.9	18.7	19.0
highway->highway	53.9	53.8	52.8	52.6	29.5	29.6	30.1	30.2
local->highway	98.1	97.4	76.9	76.1	18.1	18.2	23.1	23.4
highway->local	104.0	102.2	85.6	84.7	19.6	19.9	23.8	24.0
Average Stops				Average Number of Lane Change				
local->local	0.8	0.8	0.0	0.0	0.61	0.56	0.60	0.56
highway->highway	0.0	0.0	0.0	0.0	0.34	0.24	0.18	0.11
local->highway	0.1	0.1	0.0	0.0	1.04	0.99	1.03	0.90
highway->local	0.4	0.4	0.0	0.0	1.15	1.16	0.93	0.83

B. Sensitivity analysis with varying traffic demand levels

To test the effectiveness of the optimal control framework under different traffic conditions, we conduct simulation for a set of traffic demand levels, i.e., 10% - 200% of the existing traffic demand, and collect traffic data on the road segments between intersections 1 and 2, and between intersection 1 and the interchange. In Fig. 4, we plot the number of arrived vehicles versus total travel time by these vehicles for all the traffic demand levels under four different scenarios, with points representing the data under different demand levels. We find that, under Scenarios 1 and 2, the network operates well with any traffic demand level below 150%, where



(a) Scenario 1 vs. scenario 3



(b) Scenario 2 vs. scenario 4

Fig. 3: Vehicle following distance distribution under different scenarios.

the total travel time linearly increases with the number of arrived vehicles. When the traffic demand level is above 150%, the time spent to serve an additional 10% of vehicles increases exponentially.

The relationship between traffic flow (vehicles per hour per lane, $veh/hr-ln$) and traffic density (vehicles per km per lane, $veh/km-ln$) under different scenarios is shown in Fig. 5. The eastbound and westbound (Fig. 5a and 5b) represent local traffic between intersections 1 and 2, whereas the northbound and southbound (Fig. 5c and 5d) represent local to highway traffic between intersection 1 and the interchange. From Fig. 5, we can see that when the demand increases, the traffic gets congested in the network of uncontrolled human-driven vehicles and AVs (Scenarios 1 and 2). Especially, when

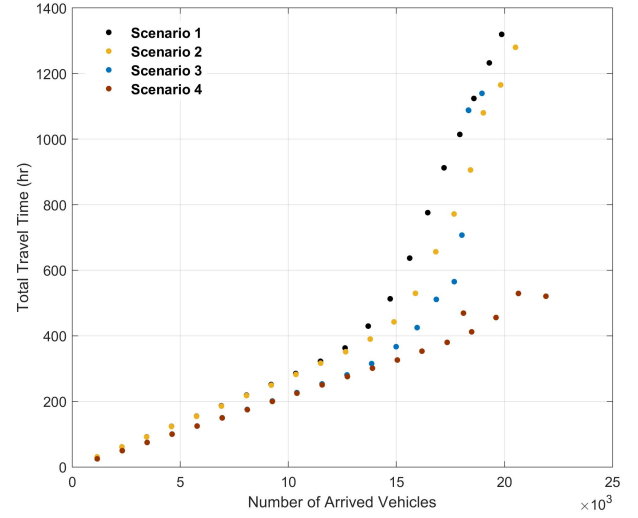


Fig. 4: Total number of arrived vehicles vs. total travel time in the network.

cycle lengths of two traffic signals are not sufficient enough to accommodate the increased traffic demand, the queues build up easily upstream the intersections and are difficult to resolve, e.g., traffic breakdown on northbound.

Under Scenario 3, traffic flow is generally improved with 1.2 s headway setting, e.g., traffic congestion is resolved for westbound and southbound directions. However, when the traffic demand is extremely high, e.g., over 2000 $veh/hr-ln$ on the northbound, it is apparent that 1.2 s headway and/or 150 m control zone length limit the extent to which network capacity could be utilized such that all the traffic demand could be satisfied. Therefore, we observe that the optimal control fails in the extreme traffic demand cases, resulting in unresolved traffic congestion, i.e., eastbound and northbound traffic under Scenario 3 in Fig. 5, and the increased travel time in as seen in Fig. 4. If, however, we take into account the capability of shorter headways for the CAVs, the optimally controlled CAVs are able to form a smooth traffic flow and eliminate congestion in the network even with the highest traffic demand level (as shown by the linear flow-density relationship under Scenario 4 in Fig. 5).

Consider that under Scenario 3, the length of control zone may not be sufficient for vehicles to adjust their acceleration/deceleration and create a 1.2 s headway between each other, we increase the control zone length

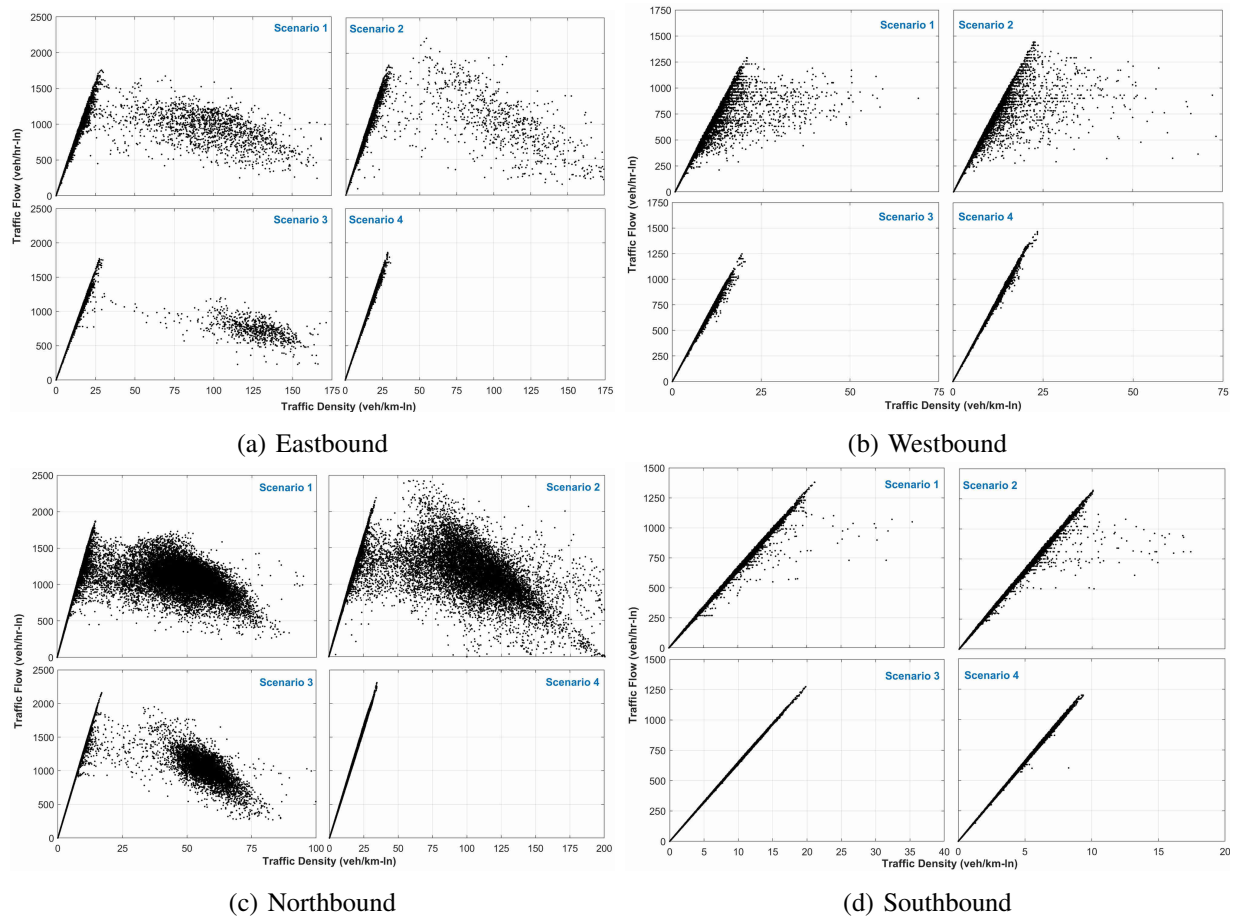


Fig. 5: Traffic flow vs. density.

to 300 m (Scenario 5) for all the conflict zones in the network, except for the unsignalized intersection nearby intersection 1 where its distance to the upstream intersection is less than 200 m . We can see that by creating a longer control zone, the overall traffic flow in the network is further enhanced (as shown in Fig. 6), especially for the northbound direction. However, the resolution of northbound traffic congestion means that more vehicles cross the intersection 1, leading to a higher traffic demand for the downstream intersections. As a result, we note that for the eastbound direction, with extremely high traffic demand, the increase of control zone length actually leads to a worse traffic congestion, i.e., larger drop in traffic flow under Scenario 5.

V. CONCLUDING REMARKS

In this paper, we compared the performance of a transportation network between optimally controlled

CAVs and uncontrolled human-driven/autonomous vehicles. The results highlight the impact of coordination of CAVs in terms of fuel economy and traffic safety. However, the control parameters of the decentralized framework need to be handled carefully to fully utilize roadway capacity and satisfy different traffic demand levels in the network.

Future research needs to be done on how to customize the parameters of the optimization framework to the intrinsic characteristics of the traffic network to be controlled to achieve the best performance. While the potential benefits of full penetration of CAVs to alleviate traffic congestion and reduce fuel consumption have become apparent, different penetrations of CAVs can alter significantly the efficiency of the entire system. Future work should focus on the interactions between CAVs and human-driven vehicles, and the influence of different market penetration of CAVs on the traffic network.

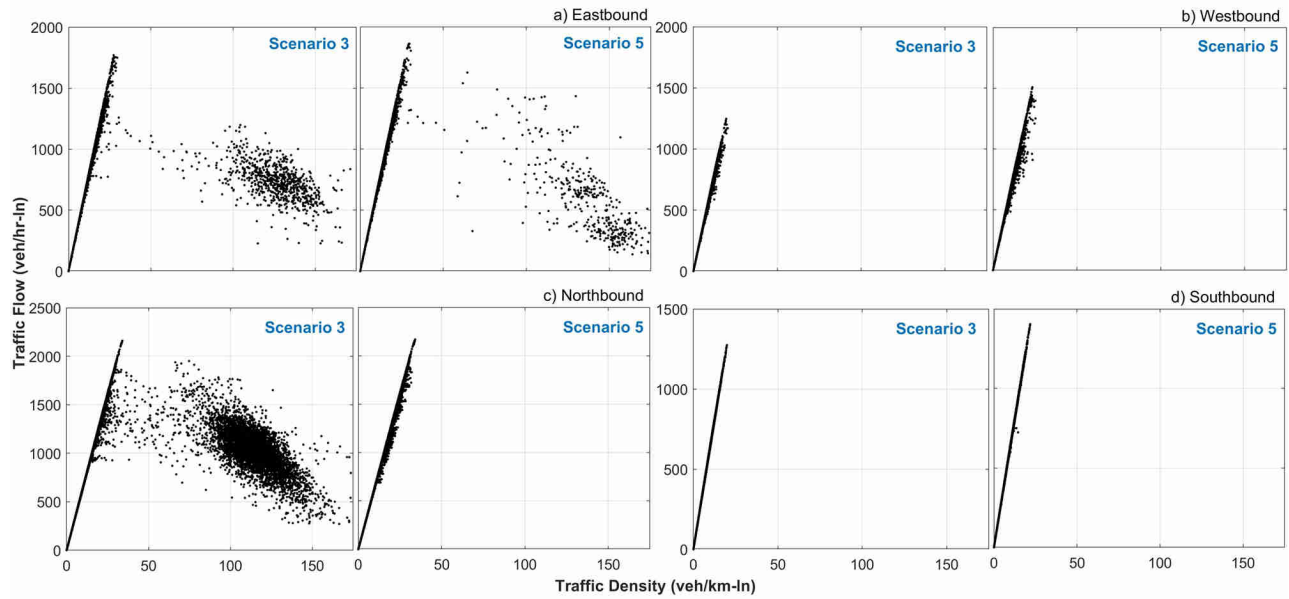


Fig. 6: Traffic flow vs. density for controlled CAVs with different control zone lengths.

ACKNOWLEDGEMENT

This manuscript has been co-authored by UT-Battelle, LLC, under contract DE-AC05-00OR22725 with the US Department of Energy (DOE). The US government retains and the publisher, by accepting the article for publication, acknowledges that the US government retains a nonexclusive, paid-up, irrevocable, worldwide license to publish or reproduce the published form of this manuscript, or allow others to do so, for US government purposes. DOE will provide public access to these results of federally sponsored research in accordance with the DOE Public Access Plan (<http://energy.gov/downloads/doepublic-access-plan>)

REFERENCES

- [1] A. A. Malikopoulos and J. P. Aguilar, "An Optimization Framework for Driver Feedback Systems," *IEEE Transactions on Intelligent Transportation Systems*, vol. 14, no. 2, pp. 955–964, 2013.
- [2] R. Margiotta and D. Snyder, "An agency guide on how to establish localized congestion mitigation programs," U.S. Department of Transportation. Federal Highway Administration, Tech. Rep., 2011.
- [3] J. Guanetti, Y. Kim, and F. Borrelli, "Control of connected and automated vehicles: State of the art and future challenges," *Annual Reviews in Control*, 2018.
- [4] P. Kachroo and Z. Li, "Vehicle merging control design for an automated highway system," in *Proceedings of Conference on Intelligent Transportation Systems*, 1997, pp. 224–229.
- [5] M. Antonioti, A. Deshpande, and A. Girault, "Microsimulation analysis of automated vehicles on multiple merge junction highways," *IEEE International Conference in Systems, Man, and Cybernetics*, pp. 839–844, 1997.
- [6] B. Ran, S. Leight, and B. Chang, "A microscopic simulation model for merging control on a dedicated-lane automated highway system," *Transportation Research Part C: Emerging Technologies*, vol. 7, no. 6, pp. 369–388, 1999.
- [7] K. Dresner and P. Stone, "Multiagent traffic management: a reservation-based intersection control mechanism," in *Proceedings of the Third International Joint Conference on Autonomous Agents and Multiagents Systems*, 2004, pp. 530–537.
- [8] —, "A multiagent approach to autonomous intersection management," *Journal of artificial intelligence research*, vol. 31, pp. 591–656, 2008.
- [9] A. de La Fortelle, "Analysis of reservation algorithms for cooperative planning at intersections," *13th International IEEE Conference on Intelligent Transportation Systems*, pp. 445–449, Sep. 2010.
- [10] S. Huang, A. Sadek, and Y. Zhao, "Assessing the Mobility and Environmental Benefits of Reservation-Based Intelligent Intersections Using an Integrated Simulator," *IEEE Transactions on Intelligent Transportation Systems*, vol. 13, no. 3, pp. 1201–1214, 2012.
- [11] I. H. Zohdy, R. K. Kamalanathsharma, and H. Rakha, "Intersection management for autonomous vehicles using iCACC," *2012 15th International IEEE Conference on Intelligent Transportation Systems*, pp. 1109–1114, 2012.
- [12] F. Yan, M. Dridi, and A. El Moudni, "Autonomous vehicle sequencing algorithm at isolated intersections," *2009 12th International IEEE Conference on Intelligent Transportation Systems*, pp. 1–6, 2009.
- [13] L. Li and F.-Y. Wang, "Cooperative Driving at Blind Crossings

- Using Intervehicle Communication,” *IEEE Transactions in Vehicular Technology*, vol. 55, no. 6, pp. 1712–1724, 2006.
- [14] F. Zhu and S. V. Ukkusuri, “A linear programming formulation for autonomous intersection control within a dynamic traffic assignment and connected vehicle environment,” *Transportation Research Part C: Emerging Technologies*, 2015.
 - [15] J. Wu, F. Perronnet, and A. Abbas-Turki, “Cooperative vehicle-actuator system: a sequence-based framework of cooperative intersections management,” *Intelligent Transport Systems, IET*, vol. 8, no. 4, pp. 352–360, 2014.
 - [16] K.-D. Kim and P. Kumar, “An MPC-Based Approach to Provable System-Wide Safety and Liveness of Autonomous Ground Traffic,” *IEEE Transactions on Automatic Control*, vol. 59, no. 12, pp. 3341–3356, 2014.
 - [17] J. Lee and B. Park, “Development and Evaluation of a Cooperative Vehicle Intersection Control Algorithm Under the Connected Vehicles Environment,” *IEEE Transactions on Intelligent Transportation Systems*, vol. 13, no. 1, pp. 81–90, 2012.
 - [18] J. Lee, B. B. Park, K. Malakorn, and J. J. So, “Sustainability assessments of cooperative vehicle intersection control at an urban corridor,” *Transportation Research Part C: Emerging Technologies*, vol. 32, pp. 193–206, 2013.
 - [19] Y. Zhou, M. E. Cholette, A. Bhaskar, and E. Chung, “Automated On-Ramp Merging and Gap Development with Speed Constraints – A State-Constrained Optimal Control Approach,” in *2018 Annual American Control Conference (ACC)*, 2018, pp. 4975–4982.
 - [20] J. Rios-Torres and A. A. Malikopoulos, “A Survey on Coordination of Connected and Automated Vehicles at Intersections and Merging at Highway On-Ramps,” *IEEE Transactions on Intelligent Transportation Systems*, vol. 18, no. 5, pp. 1066–1077, 2017.
 - [21] J. Rios-Torres, A. A. Malikopoulos, and P. Pisu, “Online Optimal Control of Connected Vehicles for Efficient Traffic Flow at Merging Roads,” in *2015 IEEE 18th International Conference on Intelligent Transportation Systems*, 2015, pp. 2432–2437.
 - [22] I. A. Ntousakis, I. K. Nikolos, and M. Papageorgiou, “Optimal vehicle trajectory planning in the context of cooperative merging on highways,” *Transportation Research Part C: Emerging Technologies*, vol. 71, pp. 464–488, 2016.
 - [23] J. Rios-Torres and A. A. Malikopoulos, “Automated and Cooperative Vehicle Merging at Highway On-Ramps,” *IEEE Transactions on Intelligent Transportation Systems*, vol. 18, no. 4, pp. 780–789, 2017.
 - [24] Y. Zhang, A. A. Malikopoulos, and C. G. Cassandras, “Optimal control and coordination of connected and automated vehicles at urban traffic intersections,” in *Proceedings of the American Control Conference*, 2016, pp. 6227–6232.
 - [25] A. A. Malikopoulos, C. G. Cassandras, and Y. J. Zhang, “A decentralized energy-optimal control framework for connected automated vehicles at signal-free intersections,” *Automatica*, vol. 93, pp. 244 – 256, 2018.
 - [26] L. Zhao, A. A. Malikopoulos, and J. Rios-Torres, “Optimal control of connected and automated vehicles at roundabouts: An investigation in a mixed-traffic environment,” in *15th IFAC Symposium on Control in Transportation Systems*, 2018, pp. 73–78.
 - [27] A. Stager, L. Bhan, A. A. Malikopoulos, and L. Zhao, “A scaled smart city for experimental validation of connected and automated vehicles,” in *15th IFAC Symposium on Control in Transportation Systems*, 2018, pp. 120–135.
 - [28] A. A. Malikopoulos, S. Hong, B. Park, J. Lee, and S. Ryu, “Optimal control for speed harmonization of automated vehicles,” *IEEE Transactions on Intelligent Transportation Systems*, 2018 (in press).
 - [29] L. Zhao and A. A. Malikopoulos, “Decentralized Optimal Control of Connected and Automated Vehicles in a Corridor,” in *2018 21st International Conference on Intelligent Transportation Systems (ITSC)*, 2018, pp. 1252–1257.
 - [30] J. Rios-Torres and A. A. Malikopoulos, “Impact of Partial Penetrations of Connected and Automated Vehicles on Fuel Consumption and Traffic Flow,” *IEEE Transactions on Intelligent Vehicles*, 2018 (in press).
 - [31] D. Department of Transportation, “Vehicle volume summary.” [Online]. Available: https://www.deldot.gov/Publications/manuals/traffic_counts/index.shtml
 - [32] R. Wiedemann, *Simulation des Strassenverkehrsflusses*. Institut für Verkehrswesen der Universität Karlsruhe, 1974.
 - [33] PTV, *PTV VISSIM 11 User Manual*, 2018.